Extracorporeal shock waves modulate myofibroblast differentiation of adipose-derived stem cells

Rinella, Letizia; Marano, Francesca; Berta, Laura; Bosco, Ornella; Fraccalvieri, Marco; Fortunati, Nicoletta; Frairia, Roberto; Catalano, Maria Graziella. Extracorporeal shock waves modulate myofibroblast differentiation of adipose-derived stem cells. WOUND REPAIR AND REGENERATION. 24 (2) pp: 275-286.
DOI: 10.1111/wrr.12410

Extracorporeal shockwaves modulate myofibroblast differentiation of adipose-derived stem cells

Letizia Rinella, MSc[1]; Francesca Marano, MSc[1]; Laura Berta, MD[2]; Ornella Bosco, PhD[1]; Marco Fraccalvieri MD[3]; Nicoletta Fortunati, MD[4]; Roberto Frairia, MD[1]; Maria Graziella Catalano, MD[1*]

[1]Department of Medical Sciences, University of Turin, 10126 Turin, Italy

[2]Med & Sport 2000 Srl, 10126 Turin, Italy

[3]Plastic Surgery Unit, University of Turin, 10126 Turin, Italy

[4]Oncological Endocrinology, AO Città della Salute e della Scienza di Torino, 10126 Turin, Italy.

*** Corresponding Author & Reprint Requests:** Maria Graziella Catalano, Department of Medical Sciences, University of Turin, Via Genova 3, 10126 Turin, Italy; tel. +39-0116705360; fax. +39-0116705366; mail: mariagraziella.catalano@unito.it

Short title: ESWs and myofibroblast differentiation

Keywords: fibrosis; extracorporeal shockwaves; adipose-derived stem cells; myofibroblasts; alpha smooth muscle actin.

Abstract

Mesenchymal stem cells are precursors of myofibroblasts, cells deeply involved in promoting tissue repair and regeneration. However, since myofibroblast persistence is associated with the development of tissue fibrosis, the use of tools that can modulate stem cell differentiation towards myofibroblasts is central. Extracorporeal shockwaves are transient short-term acoustic pulses first employed to treat urinary stones. They are a leading choice in the treatment of several orthopedic diseases and, notably, they have been reported as an effective treatment for patients with fibrotic sequels from burn scars. Based on these considerations, the aim of this study is to define the role of shockwaves in modulating the differentiation of human adipose-derived stem cells towards myofibroblasts. Shockwaves inhibit the development of a myofibroblast phenotype; they down-regulate the expression of the myofibroblast marker alpha smooth muscle actin and the extracellular matrix protein type I collagen. Functionally, stem cells acquire a more fibroblast-like profile characterized by a low contractility and a high migratory ability. Shockwave treatment reduces the expression of integrin alpha 11, a major collagen receptor in fibroblastic cells, involved in myofibroblast differentiation. Mechanistically, the resistance of integrin alpha 11-overexpressing cells to shockwaves in terms of alpha smooth muscle actin expression and cell migration and contraction suggests also a role of this integrin in the translation of shockwave signal into stem cell responses. In conclusion, the present *in vitro* study shows that stem cell differentiation towards myofibroblasts can be controlled by shockwaves and, consequently, sustains their use as a therapeutic approach in reducing the risk of skin and tissue fibrosis.

Introduction

Myofibroblasts increase during tissue regeneration and wound repair but their persistence is associated with the development of tissue fibrosis.[1] Myofibroblasts express the alpha-smooth muscle actin (αSMA), an actin isoform that represents the most reliable marker of the myofibroblastic phenotype.[2] Apart from fibroblasts and pericytes, mesenchymal stem cells are also precursors of myofibroblasts.[3]

Stem cell differentiation towards myofibroblasts is regulated by both chemical and mechanical factors.[4] There are several studies to show that different growth factors (e.g. TGF-β; bFGF) can modulate myofibroblast features, but there is an increasing body of evidence to support the role of mechanical forces in the development, progression and potentially in the regression of tissue fibrosis.[5]

The importance of mechanical forces in myofibroblast activation has been shown in the skin,[6] heart,[7] lung,[8] liver,[9] and kidney,[10] although their effects depend on the different kinds and amounts applied. More recently, there have been reports of human bone marrow mesenchymal stem cells adopting myofibroblast phenotype in culture that could contribute to cardiac fibrosis;[11] therefore, the use of tools that can control stem cell differentiation towards myofibroblasts is fundamental.

Extracorporeal shockwaves (ESWs), transient short-term acoustic pulses first employed to treat urinary stones,[12] are today a leading choice in the treatment of several orthopedic diseases.[13] Furthermore, the potential use of ESWs in promoting angiogenesis,[14] decreasing inflammation[15] and enhancing cell differentiation[16-20] has been underlined. In 2011, Fioramonti et al.[21] demonstrated that ESW therapy is an effective and conservative treatment for patients with aesthetic and functional sequels from burn scars. Recently it has been reported that ESW therapy degrades capsular fibrosis after insertion of silicone implants,[22] again suggesting a role for the use of ESWs in fibrotic diseases. However, no data are available about the involved mechanisms.

Therefore, the aim of this project was to study and provide insights on the effects of ESWs in the modulation of the differentiation of human adipose-derived stem cells (hASCs) towards myofibroblasts.

Materials and Methods

hASC isolation and characterization.

hASCs were isolated as described elsewhere.[17] Briefly, 5 healthy female donors (range 30–50 years, BMI<30) underwent elective liposuction after written consent and Institutional-Review Board authorization. The study was conducted according to the Declaration of Helsinki principles.

After digestion of raw lipoaspirates (50–100 ml) with 0.075% type I collagenase for 30 minutes, hASCs were separated by centrifugation (2100×g for 10 min), filtered and cultured in DMEM/F12 plus 10% FBS. hASCs at passage 4 were investigated by flow cytometry analysis for the expression of several antigens using the following phycoerythrin (PE) or fluorescein isothiocyanate (FITC)-conjugated antibodies: mouse anti-human CD13, CD14 and CD34 (BD Biosciences, Fraklin Lakes, NJ, USA); mouse anti-human CD45, CD90, CD105, and CD44 (Immunotech, Marseille, France). Ten thousand events were acquired for each surface marker on flow cytometer (EPICS XL, Coulter Corp., Hialeah, FL). In addition, surface marker expression was performed also at 3, 7, 14 and 21 days after ESW treatment (0.32 mJ/mm^2).

ESW treatment

The shock wave generator utilized for the *in vitro* experiments was a piezoelectric device (Piezoson 100, Richard Wolf, Knittlingen, Germany) especially designed for clinical use in orthopedics and traumatology. The experimental set-up was as previously reported.[17, 23] Both control and cells to be treated with ESWs were detached from vessels. Aliquots of 1 ml of cell suspension adjusted to 1 x 10^6cell/ml were placed in 20 mm polypropylene tubes (Nunc, Wiesbaden, Germany) and completely filled with the culture medium. Subsequently, cells were gently pelleted by centrifugation at 250 x *g* in order to minimize motion during shock wave treatment. Each cell-containing tube was placed in vertical alignment with the focal area and was adjusted so that the central point of the focal area corresponded to the centre of the tube bottom. The shock wave unit

was kept in contact with the cell containing tube by means of a water-filled cushion. Common ultrasound gel was used as a contact medium between cushion and tube. Cells were treated at room temperature as follows: 1) control cells receiving no ESW treatment and maintained in DMEM/F12 plus 10% FBS (Basal); 2) ESW-treated cells (EFD =0.32 mJ/mm^2; peak positive pressure 90 MPa) receiving a number of 1000 pulses (frequency = 4 Hz pulse repetition rate) and maintained in DMEM/F12 plus 10% FBS (ESWs).

In addition, in selected experiments cells were treated with 10 ng/ml TGF-β1 (Sigma Saint Louis, MO, USA) alone or in combination with ESWs.

In a subset of preliminary experiments, cells were treated with different energy levels (EFD =0.22 mJ/mm^2, 1000 pulses; EFD =0.32 mJ/mm^2, 1000 pulses; EFD =0.59 mJ/mm^2, 250 pulses).

After treatment, cells viability was assayed with trypan blue dye exclusion.

Cell growth

After ESW treatment, cell growth was evaluated seeding 3×10^3 cells/well in 96-well plates (Corning, New York, NY, USA). At 3, 6 and 10 days, cell viability was assessed using the Cell Proliferation Reagent WST-1 (Roche Applied Science, Penzberg, Germany), following the manufacturer's instructions. This is a colorimetric assay for the quantification of cell viability and proliferation, based on cleavage of the tetrazolium salt WST-1 by mitochondrial dehydrogenases in viable cells. Briefly, 10 µl of WST-1 were added to each well. After a 1-h incubation, absorbance at 450 nm was measured using a plate reader (Model 680 Microplate Reader; Bio-Rad, Hercules, CA, USA). Four replicate wells were used to determine each data point.

Osteogenic and adipogenic differentiation induction

To induce osteo-differentiation, hASCs were cultured in DMEM/F12 plus 10% FBS, supplemented with 10mM glycerol-2-phosphate, 10 nM dexamethasone, 150 µM ascorbic acid-2-phosphate and 10 nM cholecalciferol,[17] in the presence or absence of ESWs. After 28 days, cells were stained with

Alizarin Red S (Sigma, Saint Louis, MO, USA) for calcium deposits[17], observed under inverted microscope Leica DMI 3000 B (Leica Microsystems, Wetzlar, Germany) and photographed by Leica DCF310 FX digital camera system (Leica Microsystems., Wetzlar, Germany) at x 200 final magnification. Adipogenic differentiation was induced culturing hASCs in DMEM/F12 plus 10% FBS supplemented with 15 mM HEPES, 33 μM biotin, 17 μM pantothenate, 10 μg/ml transferrin, 5 μg/ml human insulin, 1 μM dexamethasone and 0.5 mM isobutyl-methylxanthine,[24] in the presence or absence of ESWs. After 28 days, cells were stained with Oil Red O (Sigma, Saint Louis, MO, USA) for neutral triglycerides and lipids,[24] observed under inverted microscope Leica DMI 3000 B (Leica Microsystems, Wetzlar, Germany) and photographed by Leica DCF310 FX digital camera system (Leica Microsystems., Wetzlar, Germany) at x 200 final magnification.

Colony-forming unit-fibroblast assay

After ESW treatment, cells were seeded (250 cells/well) into 24-well plates. Cells were then cultured for 10 days and subsequently fixed in methanol and stained with crystal violet. The colonies were then counted and photographed with Kodak 1 D Image equipment.

Gene expression

At 72 hours after treatments, total RNA was extracted using TRIzol Reagent (Invitrogen Ltd, Paisley, UK). DNase I was added to remove remaining genomic DNA. 1 μg of total RNA was reverse-transcribed with iScript cDNA Synthesis Kit (Bio-Rad Laboratories Inc., Hercules, CA, USA), following manufacturer' protocol. Primers (Table S1) were designed using Beacon Designer 5.0 software according to parameters outlined in the Bio-Rad iCycler Manual. Specificity of primers was confirmed by BLAST analysis. Real-time PCR was performed using a BioRad iQ iCycler Detection System (Bio-Rad Laboratories Inc., Hercules, CA, USA) with SYBR green fluorophore. Reactions were performed in a total volume of 25 μl containing 12.5 μl IQ SYBR Green Supermix (Bio-Rad Laboratories Inc., Hercules, CA, USA), 1 μl of each primer at 10 μM

concentration, and 5 μl of the previously reverse-transcribed cDNA template. The protocol used is as follows: denaturation (95°C for 5 min), amplification repeated 40 times (95°C for 15 sec, 60°C for 30 sec). A melting curve analysis was performed following every run to ensure a single amplified product for every reaction. All reactions were carried out at least in triplicate for each sample. Results were normalized using the geometric mean for three different housekeeping genes (β-actin, RPLPO and L13A) and expressed as relative expression fold *versus* untreated controls (Basal).

Immunoblotting

At different times after treatments, cells were scraped from the flask in the presence of 1 ml lysis buffer (50 mM Tris–HCl pH 7.5, 150 mM NaCl, 1 mM EDTA, 1 mM EGTA, 0.5% sodium deoxycholate, 1% Nonidet P-40, 0.1% SDS, 10 mg/ml PMSF, 30 μl/ml aprotinin and 100 mM sodium orthovanadate). Cell lysates were incubated in ice for 30–60 min. At completion, tubes were centrifuged at 4 °C for 20 min at 15,000 × g. Clear supernatants were stored at −80 °C until use. Proteins were separated on SDS-PAGE, transferred to PVDF and probed with the following antibodies: monoclonal anti-αSMA (1:1000, Sigma, Saint Louis, MO, USA); polyclonal anti-type I collagen α1 (1 μg/ml, R&D Systems, Minneapolis, MN, USA); polyclonal anti-integrin alpha 11 (1 μg/ml, R&D Systems, Minneapolis, MN, USA). The membranes were then stripped and reprobed with a rabbit polyclonal anti-GAPDH antibody (1:10000, Sigma, Saint Louis, MO, USA) to check protein loading. Proteins were detected with Pierce Super Signal chemiluminescent substrate. Bands were photographed and analyzed using Kodak 1D Image Analysis software.

Immunofluorescence microscopy

After treatments, cells (5×10^3) were seeded in 96-well plates (Corning, New York, NY, USA) for αSMA and type I collagen immunofluorescence. For ITGα11 immunofluorescence and its co-localization with vinculin, cells (1×10^5) were seeded on coverslips. After 3 and 7 days, cells were

fixed in acetone/methanol (1:1) at 4°C for 20 minutes, permeabilized with PBS containing 0.5% Triton X-100, 0.05% NaN_3 and incubated with the following antibodies: monoclonal mouse anti-αSMA (1:500, Sigma, Saint Louis, MO, USA), polyclonal sheep anti-type I collagen α1 (2 μg/ml, R&D Systems, Minneapolis, MN, USA), polyclonal goat anti-ITGα11 (2μg/ml, R&D Systems, Minneapolis, MN, USA) and monoclonal mouse anti-vinculin (1:500, Sigma, Saint Louis, MO, USA), at 4°C overnight. Detection with secondary antibodies, was as follows: for αSMA, anti-mouse conjugated with cy3 (1:10000, GE Healthcare Europe, GmbH, Milan, Italy); for collagen I, anti-sheep conjugated with Alexa Fluor 594 (1:500, Invitrogen, San Diego, CA, USA); for ITGα11, anti-goat conjugated with Alexa Fluor 594 (1:1000, Invitrogen, San Diego, CA, USA); for vinculin, anti-mouse conjugated with Alexa Fluor 488 (1:1000, Invitrogen, San Diego, CA, USA).

Nuclear staining was obtained by treating cells with Hoechst 33258 (500ng/ml in DMSO) in PBS. For αSMA and collagen, cells were observed by inverted microscope Leica DMI 4000 B (Leica Microsystems, Wetzlar, Germany) and photos of single channels and overlayers at x 200 and x 400 magnifications, were taken by Leica DCF340 FX digital camera system (Leica Microsystems, Wetzlar, Germany). For co-localization of ITGα11 and vinculin, the coverslips were mounted with Fluoromount Aqueous Mounting Medium (Sigma, Saint Louis, MO, USA) on cover glasses and images were acquired using a Zeiss Axiovert 200 M with Apotome module (Carl Zeiss Meditec, Jena, Germany), photos were taken at x 630.

Cell Contraction Assay

The Cell Contraction Assay kit (Cell Biolabs, San Diego, CA, USA) was used. Briefly, at 72 hours after treatments, one volume of untreated (Basal) and ESW-treated cell suspension (1 x 10^5 cells/well) was mixed with four volumes of collagen gel lattice mixture, plated into wells of 24-well plates, and incubated for a further 48 hours at 37°C according to the manufacturer's protocol. Gel lattices were then released from the sides of wells and the diameter of the gels was then measured at

15, 30 and 60 minutes. The extent of gel contraction was calculated by subtraction of the diameter at each time point from the initial diameter.

Scratch wound assay

After treatment, hASCs were plated onto six-well plates ($2x10^5$ cells per well). After a further 72 hours, cell monolayers were carefully wounded by scratching with a sterile plastic pipette tip. For each wound, at 0, 6 and 24 hours respectively, the photographs were taken in the same field. The distance between the wound edges was analyzed using the ImageJ 1.42 program. The percentage of wound occupied was calculated by dividing the non-recovered area at 6 and 24 hours by the initial wound area at 0 h and subtracting this value as a percentage from 100%.

Matrigel invasion assay

Cell invasion was determined using BD Biocoat Matrigel Invasion Chamber (BD Biosciences, Bedford, MA, USA). After 72 hours from ESW treatment, 5×10^4 cells were placed in the upper chamber of a transwell in the presence of 1% FBS. The bottom chamber was filled with 0.6 ml DMEM/F12 plus 10% FBS as a chemo attractant. After a further 24 hours, cells on the upper side of the insert were removed with cotton swabs, membranes fixed in methanol and cells stained with crystal violet and photographed. The number of cells that had migrated to the basal side of the membrane was quantified by counting 12 independent fields under the microscope.

ITGα11 transfection

Cells ($2.5x10^5$ cells/well) were transfected with 2.5 μg of plasmid DNA encoding for ITGα11 (OriGene Technologies, Rockville, MD, USA) using 7.5 μl Lipofectamine 2000™ (Invitrogen Ltd, Paisley, UK), either in the presence or absence of ESWs treatment. After further 48h, cells were used for contraction and scratch wound assays as above. Moreover, after 72 hours, RNA was extracted and used to determine ITGα11 and αSMA expression.

Statistical Analyses

Data are expressed throughout the text as means ± SD, calculated from at least three different experiments. Comparison between groups was performed with analysis of variance (one-way ANOVA) and the threshold of significance was calculated with the Bonferroni test. Comparison between ESW-treated and untreated cells was performed with Student t-test. Statistical significance was set at $p<0.05$.

Results

hASC characterization

As shown in Table 1, hASCs expressed mesenchymal stem cell markers CD13 (97.2%), CD44 (98.8%), CD90 (92.6%) and CD105 (96.5%), whereas a very low expression of CD14 (1-4%) and no expression of CD34 and CD45 were detected. Their expression remained unchanged up to 21 days, both in basal conditions and after ESW treatment at 0.32 mJ/mm^2. ESW permitted a cell viability > 85% (data not shown), and it did not affect cell growth up to 10 days (Figure 1, panel A). As expected, hASCs were able to differentiate into osteogenic and adipogenic lineages (Figure 1, panel B) under specific culture conditions, confirming their differentiating potential. ESW treatment further increased the osteogenic potential, as we already reported elsewhere[17].

ESW effect on clonogenicity and self-renewal

As shown in Figure 1, panel C, hASCs were able to form colonies, but ESW treatment did not change the number of colony-forming units (CFU). As well, ESWs did not modify the expression of self-renewal markers (Figure 1, panel D).

ESW effect on αSMA expression

ESWs determined a significant reduction in αSMA gene expression, being its expression reduced to 0.76 by the treatment at 0.22 mJ/mm^2 ($p<0.01$), to 0.22 by the treatment at 0.32 mJ/mm^2 ($p<0.001$), and to 0.33 by the treatment at 0.59 mJ/mm^2 ($p<0.001$), respectively (Figure 2, panel A). Since the best reduction was obtained with an energy level of 0.32 mJ/mm^2 this treatment schedule was chosen for further experiments. The reduction in gene expression resulted in a reduction in cells expressing αSMA protein, as determined by immunofluorescence (Figure 2, panel B); moreover, the protein level was significantly reduced up to 14 days from ESW treatment ($p<0.001$ for all time points), as revealed by western blot analysis (Figure 2, panels C and D).

ESW effect on collagen production

Myofibroblasts primarily deposit collagen, whose excessive production is considered a hallmark of tissue fibrosis.[4] ESWs significantly reduced the expression of type I collagen α1 to 0.51 ($p<0.01$; Figure 3, panel A) and of type I collagen α2 to 0.10 ($p<0.001$; Figure 3, panel B) as well as the expression of type V collagen α1 to 0.58 ($p<0.01$Figure 3, panel C) and of type V collagen α2 to 0.29 ($p<0.001$; Figure 3, panel D). The latter is found in tissues containing type I collagen and appears to regulate the assembly of heterotypic fibers composed of both type I and type V collagen.[25] The reduction in type I collagen gene expression determined a reduction at a protein level, as demonstrated by both immunofluorescence (Figure 3, panel E) and western blotting (Figure 3, panel F and G, $p<0.001$)

ESW effect on cell contraction and migration

Functionally, myofibroblasts are characterized by high contractility and low migration potential.[26] To assess the effect of ESWs on contractility of hASCs, a gel contraction assay was used. As shown in Figure 4, panels A and B, ESWs significantly impaired cell contractility. Migration of hASCs was significantly increased by ESW treatment as revealed by both scratch wound (Figure 5, panels A and B) and matrigel invasion (Figure 5, panels C and D) assays. After 6 hours from scratch, ESW-treated hASCs occupied 33% of the wound with respect to 16% occupation of untreated cells ($p< 0.01$); after 24 hours, ESW-treated cells occupied 67% of the wound with respect to 41% occupation of untreated cells ($p<0.01$). The trans-well invasion chamber further confirmed the increase of cell migration. The number of invading cells per field increased from 12.7 to 47 at 24 hours after ESW treatment ($p<0.001$).

ESW effect on integrin expression

As integrins are known to play a key role in mechanotransduction,[27] we analyzed the effect of ESW treatment on gene expression of integrins α3, α5, αv and α11 that have been suggested to be central

mediators of fibrosis in multiple organs.[28] As reported in Figure 6, ESWs determined a significant reduction in integrin α11 (panel A, $p<0.001$), whereas no significant modulation was observed in the expression of integrins α3, α5, αv (data not shown). The reduction in integrin α11 gene expression translated into a protein level reduction, as revealed by western blotting (Figure 6, panel B and C) and immunofluorescence (Figure 6, panel D). In addition, as shown in Figure 6 panel D, co-staining with vinculin supported ITGα11 localization in focal adhesions.

To further support a role of ITGα11 in the translation of ESW signal into hASC response, we demonstrated that overexpressing ITGα11 cells (Figure 7, panel A) were less sensitive to ESW in terms of αSMA expression (Figure 7, panel B), cell contraction (Figure 7, panel C) and migration (Figure 7, panel D).

ESW effect on TGF-β1 induced αSMA expression

As it was recently reported that TGF-β1 stimulated the expression of αSMA in hASCs,[29] we investigated the effects of combining TGF-β1 with ESWs. Also in our *in vitro* model, TGF-β1 increased the expression of αSMA, while ESWs completely abolished the effect of this growth factor in terms of both mRNA (Figure 8, panel A) and protein level (Figure 8, panels B and C) of αSMA.

Discussion

The present paper delineates for the first time the ability of ESWs to modulate the differentiation of hASCs towards myofibroblasts with important implications for the treatment of tissue fibrosis.

We isolated hASCs from healthy donor lipoaspirates; these cells expressed mesenchymal stem cell markers and were able to differentiate into osteogenic and adipogenic lineages, confirming them as a good stem cell model. Our ESW schedule did not affect cell growth, thus permitting good viability and cell performance. As we already reported elsewere,[17] ESW treatment further increased the osteogenic differentiating potential of hASCs, but it did not change their clonogenicity and stemness abilities. Quite recently, other groups reported that ESWs increase differentiation potential of mesenchymal stem cells[18-20]; however, this could be in part due to the use of different ESW generators, treatment schedules, species and stem cell sources. Although some recent literature suggests the use of a water bath to apply shockwaves to cell cultured in flasks,[30] we applied ESWs directly to cell suspension containing tubes to avoid the non-homogeneous effects resulting from treatment of monolayer cells in flasks. In fact, it is reported that when treating cells in flasks, there are signs of significant cell detachment and injury close to the focus region.[31] ESW dosage is higher at the center of the culture where cells may be damaged and eventually undergo apoptosis; on the contrary, cells at the edges receiving a lower dose are positively stimulated to proliferation and differentiation.[32]

Here, we demonstrated that biochemical and biological functions, associated with myofibroblast phenotype, can be decreased through ESW treatment. The generation of contractile forces is primarily associated with the expression of αSMA, an actin form linked to the differentiation of myofibroblasts.[4] Our hASCs expressed αSMA accordingly with previous reports,[33] and in our experimental conditions ESWs determined a significant reduction of αSMA, both in terms of gene

expression as well as protein production. This reduction was observed at all energy levels used and lasted for at least 14 days from treatment.

To date, there are no studies available on the effects of ESWs on αSMA expression and there are contradictory results on the effects of mechanical forces. Indeed, some studies reported the positive effect of mechanical forces on αSMA expression;[34,35] on the contrary, others revealed a negative effect.[35,36] Uniaxial strain determined a reduction of αSMA in hASCs;[36] in bone marrow stem cells, cyclic equiaxial strain down-regulated αSMA whereas cyclic uniaxial strain transiently increased its expression.[37] Furthermore, it is reported that the effect of forces depends on the basal level of αSMA.[38] Our cells expressed a good level of αSMA; therefore our data are in agreement with the observation that in cells with an abundant αSMA level force may inhibit αSMA activity whereas in cells with low levels, force induces its expression.[38]

Beyond affecting αSMA expression, ESWs determined the reduction of type I collagen production by hASCs. Our data are in line with observations made by other authors reporting that ESWs ameliorate cardiac remodeling after infarction, by reducing collagen deposition.[39] On the other hand, as we reported elsewhere, ESWs increased collagen expression in fibroblasts[40] and had stimulating effects on tenocytes.[41] The different biological behaviors, at least partially, may depend upon the distinct cell types, different ESW treatment schedules, and the presence of specific growth factors.

Functionally, we found that ESW treatment inhibited collagen gel contraction of hASCs and had pro-migratory effects. Our data are in agreement with the results of Suhr and colleagues,[16] who reported that ESW treatment improved bone-marrow stem cell migration. Migration correlated with the down-regulation of αSMA. The former work of Petersen et al.[42] reported that αSMA expression leads to decreased motility, and recent work by Talele et al. suggests that αSMA expression determines the fate of MSCs.[43] Present data suggest that ESWs may mimic the effect of bFGF; even

if we couldn't find any modification in bFGF expression after ESW treatment (data not shown), the positive effect of ESWs on ERK phosphorylation, we reported elsewhere,[17] might, at least partly, explain the effect of ESWs on hASC migration. Furthermore, we here demonstrate that ESWs counteracted the effect of TGF-β, in accordance with Desai et al.[29] who recently reported that hASCs treated with TGF-β develop a myofibroblastic phenotype with an increase in αSMA expression.

Finally, we observed that ESW treatment significantly reduced the expression of integrin α11. Integrins are a large family of transmembrane adhesive proteins that influence a wide array of biologic processes including tissue organization and inflammation.[27] Integrin α11 is a major collagen receptor on fibroblastic cells;[44,45] it controls myofibroblast differentiation and it is involved in collagen reorganization mediated by myofibroblasts. As we here demonstrate that overexpressing ITGα11 cells are less sensitive to ESW in terms of αSMA expression, cell contraction and migration, we suggest a role of ITGα11 in the translation of ESW signal into hASC responses. In accordance to our results, quite recently,[46] it has been demonstrated that α11 integrin, acting through the Smad-dependent TGF-β2 signaling, may contribute to the formation of pro-fibrotic myofibroblasts and the development of a fibrotic interstitium in diabetic cardiomyopathy. Even if it has been suggested that other integrins are involved in fibrosis development, among them is the integrin αv, we did not observe any modification in α3, α5, and αv integrin expression. The expression of integrin αvβ6 has been described on type II alveolar epithelial cells of patients with idiopathic pulmonary fibrosis and scleroderma lung fibrosis.[47] The role of integrin αvβ6 in renal fibrosis, in the unilateral ureteral obstruction model and in acute biliary fibrosis has also been shown.[48,49] However, integrin αvβ6 may not be involved in all forms of fibrosis, as noted by the lack of an effect in the carbon tetrachloride (CCL4)-induced liver fibrosis model.

In conclusion, the present *in vitro* study suggests a prominent role for ESWs in modulating mesenchymal stem cells behavior during scar formation and tissue repair and gives insights into the involved mechanisms.

Acknowledgments

We thank Med & Sport 2000 S.r.l., Turin, Italy for providing the shock wave generator; Eleonora Gargantini for her technical support on adipogenic differentiation; Arturo Rosso for plasmid amplification; Cristina Grange for co-staining experiments; Gillian Lynch for English editing.

The study was supported by "Progetto Ateneo 2011", University of Turin, to Roberto Frairia and by Fondazione CRT Turin, Italy, to Maria Graziella Catalano.

The authors have declared no conflicting interests.

List of Abbreviations:

bFGF	basic fibroblast growth factor
CCL4	carbon tetrachloride
COL1A1	type I collagen α1
COL1A2	type I collagen α2
COL5A1	type V collagen α1
COL5A2	type V collagen α2
DMEM-F12	dulbecco's modified eagle medium: nutrient mixture F-12
DMSO	dimethyl sulfoxide
EDTA	ethylene diamine tetraacetic acid
EFD	energy flux density
EGTA	ethylene glycol tetraacetic acid
ERK	extracellular signal-regulated kinases
ESWs	Extracorporeal shockwaves
FBS	fetal bovine serum
FITC	fluorescein isothiocyanate
GAPDH	glyceraldehyde-3-phosphate dehydrogenase
hASCs	human Adipose-derived Stem Cells
ITGα11	integrin alpha 11
KLF4	Kruppel-like factor 4
NANOG	Nanog homeobox
NP40	nonyl phenoxypolyethoxylethanol 40
OCT4	octamer-binding transcription factor 4
PBS	phosphate buffered saline
PE	phycoerythrin
PMSF	phenyl methane sulfonyl fluoride
PPARγ	peroxisome proliferator-activated receptor gamma
PVDF	polyvinylidene difluoride
Runx2	runt-related transcription factor 2
SDS	sodium dodecyl sulfate
SOX2	SRY (sex determining region Y)-box 2

TGF-β	transforming growth factor β
αSMA	alpha-smooth muscle actin

References

1. Sarrazy V, Billet F, Micallef L, Coulomb B, Desmoulière A. Mechanisms of pathological scarring: role of myofibroblasts and current developments. *Wound Repair Regen* 2011; 19: s10-5.
2. Hinz B. Formation and function of the myofibroblast during tissue repair. *J Invest Dermatol* 2007; 127: 526–37.
3. Kramann R, DiRocco DP, Humphreys BD. Understanding the origin, activation and regulation of matrix-producing myofibroblasts for treatment of fibrotic disease. *J Pathol* 2013; 231: 273-89.
4. Tomasek JJ, Gabbiani G, Hinz B, Chaponnier C, Brown RA. Myofibroblasts and mechano-regulation of connective tissue remodelling. *Nat Rev Mol Cell Biol* 2002; 3: 349-63.
5. Wells RG. Tissue mechanics and fibrosis. *Biochim Biophys Acta* 2013; 1832: 884-90.
6. Squier CA. The effect of stretching on formation of myofibroblasts in mouse skin. *Cell Tissue Res* 1981; 220: 325-35.
7. Galie PA, Westfall MV, Stegemann JP. Reduced serum content and increased matrix stiffness promote the cardiac myofibroblast transition in 3D collagen matrices. *Cardiovasc Pathol* 2011; 20: 325-33.
8. Balestrini JL, Chaudhry S, Sarrazy V, Koehler A, Hinz B. The mechanical memory of lung myofibroblasts. *Integr Biol (Camb)* 2012; 4: 410-21.
9. Li Z, Dranoff JA, Chan EP, Uemura M, Sévigny J, Wells RG. Transforming growth factor-beta and substrate stiffness regulate portal fibroblast activation in culture. *Hepatology* 2007; 46: 1246-56.
10. Cortes P, Zhao X, Riser BL, Narins RG. Role of glomerular mechanical strain in the pathogenesis of diabetic nephropathy. *Kidney Int* 1997; 51: 57-68.

11. Ngo MA, Müller A, Li Y, Neumann S, Tian G, Dixon IM, et al. Human mesenchymal stem cells express a myofibroblastic phenotype in vitro: comparison to human cardiac myofibroblasts. *Mol Cell Biochem* 2014; 392: 187-204.
12. Sturtevant B. Shock waves physic of lithotripters. In: Smith A, Badlani GH, Bagley DH, editors. Smith's Textbook of endourology. St Louis, MO, Quality Medical Publishing; 1996. pp. 529-552.
13. Wang CJ. Extracorporeal shockwave therapy in musculoskeletal disorders. *J Orthop Surg Res* 2012; **7**: 11.
14. Mittermayr R, Hartinger J, Antonic V, Meinl A, Pfeifer S, Stojadinovic A, et al. Extracorporeal shock wave therapy (ESWT) minimizes ischemic tissue necrosis irrespective of application time and promotes tissue revascularization by stimulating angiogenesis. *Ann Surg* 2011; 253: 1024-32.
15. Davis TA, Stojadinovic A, Anam K, Amare M, Naik S, Peoples GE, et al. Extracorporeal shock wave therapy suppresses the early proinflammatory immune response to a severe cutaneous burn injury. *Int Wound J* 2009; 6: 11-21.
16. Suhr F, Delhasse Y, Bungartz G, Schmidt A, Pfannkuche K, Bloch W. Cell biological effects of mechanical stimulations generated by focused extracorporeal shock wave applications on cultured human bone marrow stromal cells. *Stem Cell Res* 2013; 11: 951-64.
17. Catalano MG, Marano F, Rinella L, de Girolamo L, Bosco O, Fortunati N, et al. Extracorporeal shockwaves (ESWs) enhance the osteogenic medium-induced differentiation of adipose-derived stem cells into osteoblast-like cells. *J Tissue Eng Regen Med* 2014 Jun 1. doi: 10.1002/term.1922.

18. Schuh CM, Heher P, Weihs AM, Banerjee A, Fuchs C, Gabriel C, et al. In vitro extracorporeal shock wave treatment enhances stemness and preserves multipotency of rat and human adipose-derived stem cells. *Cytotherapy* 2014; 16:1666-78.

19. Sun D, Junger WG, Yuan C, Zhang W, Bao Y, Qin D, et al. Shockwaves induce osteogenic differentiation of human mesenchymal stem cells through ATP release and activation of P2X7 receptors. *Stem Cells* 2013; 31: 1170-80.

20. Raabe O, Shell K, Goessl A, Crispens C, Delhasse Y, Eva A, et al. Effect of extracorporeal shock wave on proliferation and differentiation of equine adipose tissue-derived mesenchymal stem cells in vitro. *Am J Stem Cells* 2013; 2: 62-73.

21. Fioramonti P, Cigna E, Onesti MG, Fino P, Fallico N, Scuderi N. Extracorporeal shock wave therapy for the management of burn scars. *Dermatol Surg* 2012; 38: 778-82.

22. Fischer S, Mueller W, Schulte M, Kiefer J, Hirche C, Heimer S, et al. Multiple extracorporeal shock wave therapy degrades capsular fibrosis after insertion of silicone implants. *Ultrasound Med Biol* 2015; 41: 781-9.

23. Frairia R, Catalano MG, Fortunati N, Fazzari A, Raineri M, Berta L. High energy shock waves (HESW) enhance paclitaxel cytotoxicity in MCF-7 cells. *Breast Cancer Res Treat* 2003; 81: 11-19.

24. Granata R, Gallo D, Luque RM, Baragli A, Scarlatti F, Grande C, et al. Obestatin regulates adipocyte function and protects against diet-induced insulin resistance and inflammation. *FASEB J.* 2012; 26: 3393-411.

25. Sun M, Chen S, Adams SM, Florer JB, Liu H, Kao WW, et al. Collagen V is a dominant regulator of collagen fibrillogenesis: dysfunctional regulation of structure and function in a corneal-stroma-specific Col5a1-null mouse model. *J Cell Sci* 2011; 124: 4096-105.

26. Majno G, Gabbiani G, Hirschel BJ, Ryan GB, Statkov PR. Contraction of granulation tissue in vitro: similarity to smooth muscle. *Science* 1971; 173: 548–50.
27. Goldmann WH. Mechanotransduction in cells. *Cell Biol Int* 2012; 36: 567-70.
28. Agarwal SK. Integrins and cadherins as therapeutic targets in fibrosis. *Front Pharmacol* 2014; 5: 131.
29. Desai VD, Hsia HC, Schwarzbauer JE. Reversible modulation of myofibroblast differentiation in adipose-derived mesenchymal stem cells. *PLoS One* 2014; 9: e86865.
30. Holfeld J, Tepeköylü C, Kozaryn R, Mathes W, Grimm M, Paulus P. Shock wave application to cell cultures. *J Vis Exp* 2014; 86.
31. Sondén A, Johansson AS, Palmblad J, Kjellström BT. Proinflammatory reaction and cytoskeletal alterations in endothelial cells after shock wave exposure. *J Investig Med* 2006; 54: 262-71.
32. Tamma R, dell'Endice S, Notarnicola A, Moretti L, Patella S, Patella V, et al. Extracorporeal shock waves stimulate osteoblast activities. *Ultrasound Med Biol* 2009; 35: 2093-100.
33. Ryu YJ, Cho TJ, Lee DS, Choi JY, Cho J. Phenotypic characterization and in vivo localization of human adipose-derived mesenchymal stem cells. *Mol Cells* 2013; 35: 557-64.
34. Hinz B, Mastrangelo D, Iselin CE, Chaponnier C, Gabbiani G. Mechanical tension controls granulation tissue contractile activity and myofibroblast differentiation. *Am J Pathol* 2001; 159:1009-20.
35. Riha GM, Wang X, Wang H, Chai H, Mu H, Lin PH, et al. Cyclic strain induces vascular smooth muscle cell differentiation from murine embryonic mesenchymal progenitor cells. *Surgery* 2007; 141: 394-402.
36. Park JS, Chu JS, Cheng C, Chen F, Chen D, Li S. Differential effects of equiaxial and uniaxial strain on mesenchymal stem cells. *Biotechnol Bioeng* 2004; 88: 359-68.

37. Lee WC, Maul TM, Vorp DA, Rubin JP, Marra KG. Effects of uniaxial cyclic strain on adipose-derived stem cell morphology, proliferation, and differentiation. *Biomech Model Mechanobiol* 2007; 6: 265-73.

38. Wang J, Seth A, McCulloch CA. Force regulates smooth muscle actin in cardiac fibroblasts. *Am J Physiol Heart Circ Physiol* 2000; 279: H2776-85.

39. Lei PP, Tao SM, Shuai Q, Bao YX, Wang SW, Qu YQ, Wang DH. Extracorporeal cardiac shock wave therapy ameliorates myocardial fibrosis by decreasing the amount of fibrocytes after acute myocardial infarction in pigs. *Coron Artery Dis* 2013; 24: 509-15.

40. Berta L, Fazzari A, Ficco AM, Enrica PM, Catalano MG, Frairia R. Extracorporeal shock waves enhance normal fibroblast proliferation in vitro and activate mRNA expression for TGF-beta1 and for collagen types I and III. *Acta Orthop* 2009; 80:612-7.

41. Vetrano M, d'Alessandro F, Torrisi MR, Ferretti A, Vulpiani MC, Visco V. Extracorporeal shock wave therapy promotes cell proliferation and collagen synthesis of primary cultured human tenocytes. *Knee Surg Sports Traumatol Arthrosc* 2011; 19: 2159-68.

42. Rønnov-Jessen L, Petersen OW. A Function for Filamentous a-Smooth Muscle Actin: Retardation of Motility in Fibroblasts. *J Cell Biol* 1996; 134: 67-80.

43. Talele NP, Fradette J, Davies JE, Kapus A, Hinz B. Expression of α-Smooth Muscle Actin Determines the Fate of Mesenchymal Stromal Cells. *Stem Cell Reports* 2015; 4: 1016-1030.

44. Velling T, Kusche-Gullberg M, Sejersen T, Gullberg D. cDNA cloning and chromosomal localization of human a11 integrin. A collagen-binding, I domain-containing, b1-associated integrin a-chain present in muscle tissues. *J Biol Chem* 1999; 274: 25735–42.

45. Popova SN, Barczyk M, Tiger CF, Beertsen W, Zigrino P, Aszodi A, et al. Alpha11 beta1 integrin-dependent regulation of periodontal ligament function in the erupting mouse incisor. *Mol Cell Biol* 2007; 27: 4306–16.

46. Talior-Volodarsky I, Connelly KA, Arora PD, Gullberg D, McCulloch CA. α11 integrin stimulates myofibroblast differentiation in diabetic cardiomyopathy. *Cardiovasc Res* 2012; 96: 265-75.

47. Horan GS, Wood S, Ona V, Li DJ, Lukashev ME, Weinreb PH, et al. Partial inhibition of integrin alpha(v)beta6 prevents pulmonary fibrosis without exacerbating inflammation. *Am J Respir Crit Care Med* 2008; 177: 56-65.

48. Ma LJ, Yang H, Gaspert A, Carlesso G, Barty MM, Davidson JM, et al. Transforming growth factor-beta-dependent and -independent pathways of induction of tubulointerstitial fibrosis in beta6(-/-) mice. *Am J Pathol* 2003; 163: 1261-73.

49. Wang B, Dolinski BM, Kikuchi N, Leone DR, Peters MG, Weinreb PH, et al. Role of alphavbeta6 integrin in acute biliary fibrosis. *Hepatology* 2007; 46: 1404-12.

Figure Legends

Figure 1. ESW effect on cell growth (A). Cell growth up to ten days after ESW treatment was assessed by WST-1 assay. **Osteogenic and adipogenic differentiation of hASCs (B).** Alizarin, Oil Red O staining and expression of Rux2 and PPARγ of hASCs treated with ESWs and either osteogenic or adipogenic media, respectively. Magnification, *x 200*. **CFU formation (C).** Clonogenicity was assessed by counting the number of colonies after ESW treatment. **Self-renewal marker expression (D).** mRNA expression of SOX2, OCT4, KLF4 and NANOG after ESW treatment.

Figure 2. ESW effect on αSMA expression. mRNA expression of αSMA (A) at 72 hours after treatment with ESWs at different energy levels (0.22; 0.32, 0.59 mJ/mm^2). Results are normalized for three different housekeeping genes (β-actin, RPLPO and L13A) and expressed as relative expression fold *vs* Basal. Significance *vs* basal: **, p<0.01; ***, p<0.001; significance *vs* 0.32 mJ/mm^2: °°°, p<0.001. Immunofluorescence for αSMA (B) at 72 hours after ESW treatment (0.32 mJ/mm^2, 1000 pulses). Magnification, *x 200*. Inset: magnification, *x 400*. Immunoblotting for αSMA (C) at 3, 7 and 14 days after ESW treatment (0.32 mJ/mm^2, 1000 pulses). Anti-GAPDH was used to confirm equal loading. Blot is representative of three independent experiments. Semiquantitative analysis of immunoblotting results (D). Significance vs cells in basal conditions: ***, p<0.001.

Figure 3. ESW effect on collagen production. mRNA expression of COL1A1 (A); COL1A2 (B); COL5A1 (C); COL5A2 (D) at 72 hours after ESW treatment (0.32mJ/mm^2, 1000 pulses). Results are normalized for three different housekeeping genes (β-actin, RPLPO and L13A) and expressed as relative expression fold vs basal. Significance vs Basal: **, p<0.01; ***, p<0.001. Immunofluorescence for type I collagen (E) at 7 days after ESW treatment (0.32 mJ/mm^2, 1000 pulses). Magnification, *x 200*. Immunoblotting for type I collagen (F) at 7 days after ESW

treatment. Anti-GAPDH was used to confirm equal loading. Blot is representative of three independent experiments. Semiquantitative analysis of immunoblotting results (G). Significance vs cells in basal conditions: ***, $p<0.001$.

Figure 4. ESW effect on cell contraction. Contraction inhibition (A) by ESWs of hASCs in collagen gel lattice. The change in gel size (diameter) was measured up to 60 min after release. Gel matrices (n= 2) in Basal conditions and after ESW treatment, imaged at 60 min time point (B).

Figure 5. Scratch wound assay after ESW treatment. Representative phase-contrast images (A) showing the position of the wound edges at 0, 6 and 24 hours after scratching. Percentage of wound occupied (B), calculated by dividing the non-recovered area at 6 and 24 hours by the initial wound area at 0 h and subtracting this value as a percentage from 100%. Significance vs cells in basal conditions: **, $p<0.01$. **Invasion assay after ESW treatment.** Representative phase-contrast images showing invading cells at 24 hours after ESW treatment (0.32mJ/mm^2, 1000 pulses), using a Transwell migration assay (C). Number of cells/field invading the lower surfaces of the filter was counted (D). Significance *vs* cells in basal conditions: ***, $P<0.001$.

Figure 6. ESW effect on integrin expression. mRNA expression of ITGα11 (A) at 72 hours after ESW treatment (0.32mJ/mm^2, 1000 pulses). Results are normalized for three different housekeeping genes (β-actin, RPLPO and L13A) and expressed as relative expression fold vs Basal. Immunoblotting for ITGα11 (B) at 72 hours after ESW treatment. Anti-GAPDH was used to confirm equal loading. Blot is representative of three independent experiments. Semiquantitative analysis of immunoblotting results (C). Significance vs cells in basal conditions: ***, $P<0.001$. Staining (D) for ITGα11(red) and vinculin (green) at 72 hours after ESW treatment (0.32 mJ/mm^2, 1000 pulses). Magnification, *x 630*.

Figura 7. ESW effect on ITGα11-overexpressing cells. ITGα11 expression (A) after ITGα11 transfection in the presence or absence of ESWs. ESW effect on αSMA expression (B); cell

contraction (C) and migration (D and F) of ITGα11-transfected cells. Significance *vs* not transfected cells (basal): ***, P<0.001.

Figure 8. Effects of TGF-β and ESWs on αSMA expression. mRNA expression of αSMA (A) at 72 hours after TGF-β and ESW treatment (0.32mJ/mm^2, 1000 pulses). Results are normalized for three different housekeeping genes (β-actin, RPLPO and L13A) and expressed as relative expression fold vs Basal. Immunoblotting for αSMA (B) at 72 hours after ESW treatment. Anti-GAPDH was used to confirm equal loading. Blot is representative of three independent experiments. Semiquantitative analysis of immunoblotting results (C). Significance vs cells in basal conditions: **, p<0.01; ***, P<0.001.

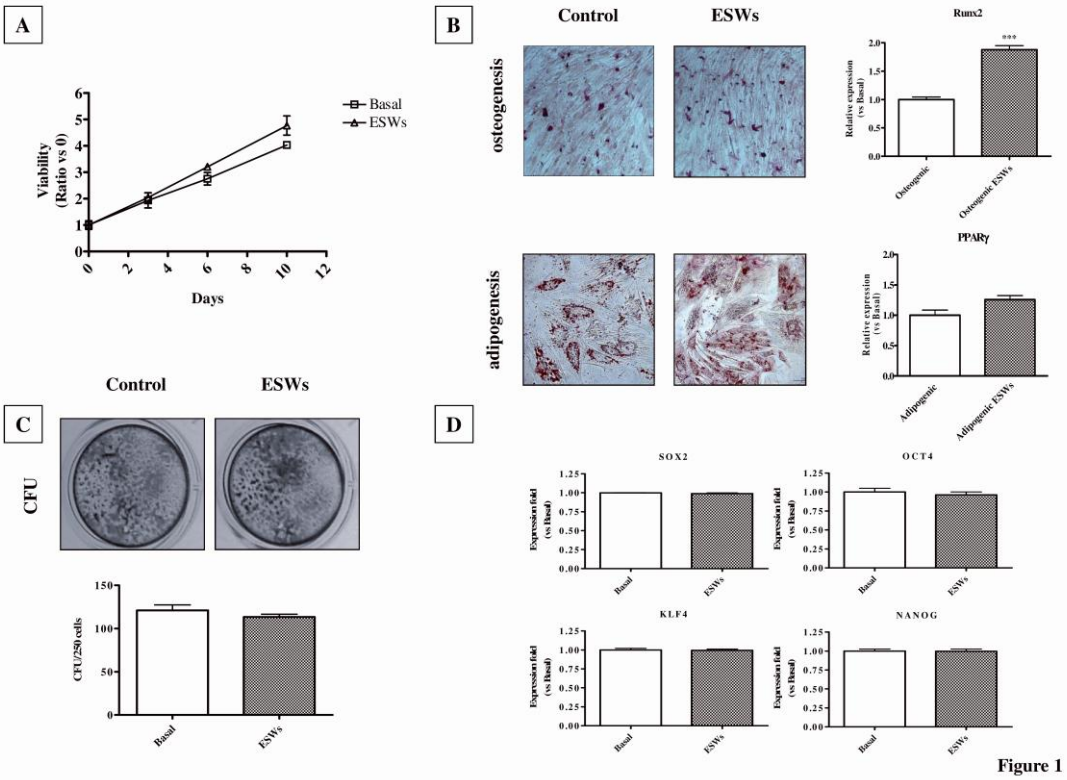
A
Viability (Ratio vs 0)
Days
Basal
ESWs
B
Control
ESWs
osteogenesis
adipogenesis
Runx2
PPARγ
Relative expression (vs Basal)
Osteogenic
Osteogenic ESWs
Adipogenic
Adipogenic ESWs
C
Control
ESWs
CFU
CFU/250 cells
Basal
ESWs
D
SOX2
OCT4
KLF4
NANOG
Expression fold (vs Basal)

Figure 1

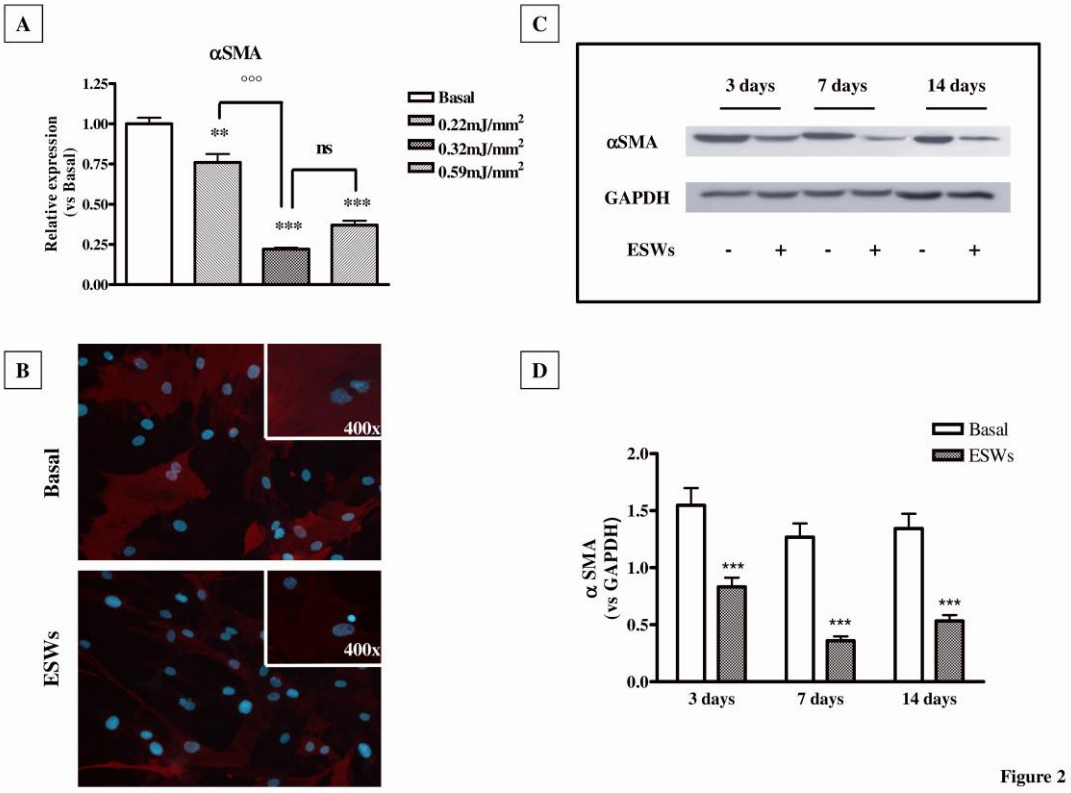
A
αSMA
Relative expression (vs Basal)
1.25
1.00
0.75
0.50
0.25
0.00
**
ns
***
***
Basal
0.22mJ/mm2
0.32mJ/mm2
0.59mJ/mm2
C
3 days
7 days
14 days
αSMA
GAPDH
ESWs - + - + - +
B
Basal
ESWs
400x
400x
D
Basal
ESWs
α SMA (vs GAPDH)
2.0
1.5
1.0
0.5
0.0
***
***
***
3 days
7 days
14 days

Figure 2

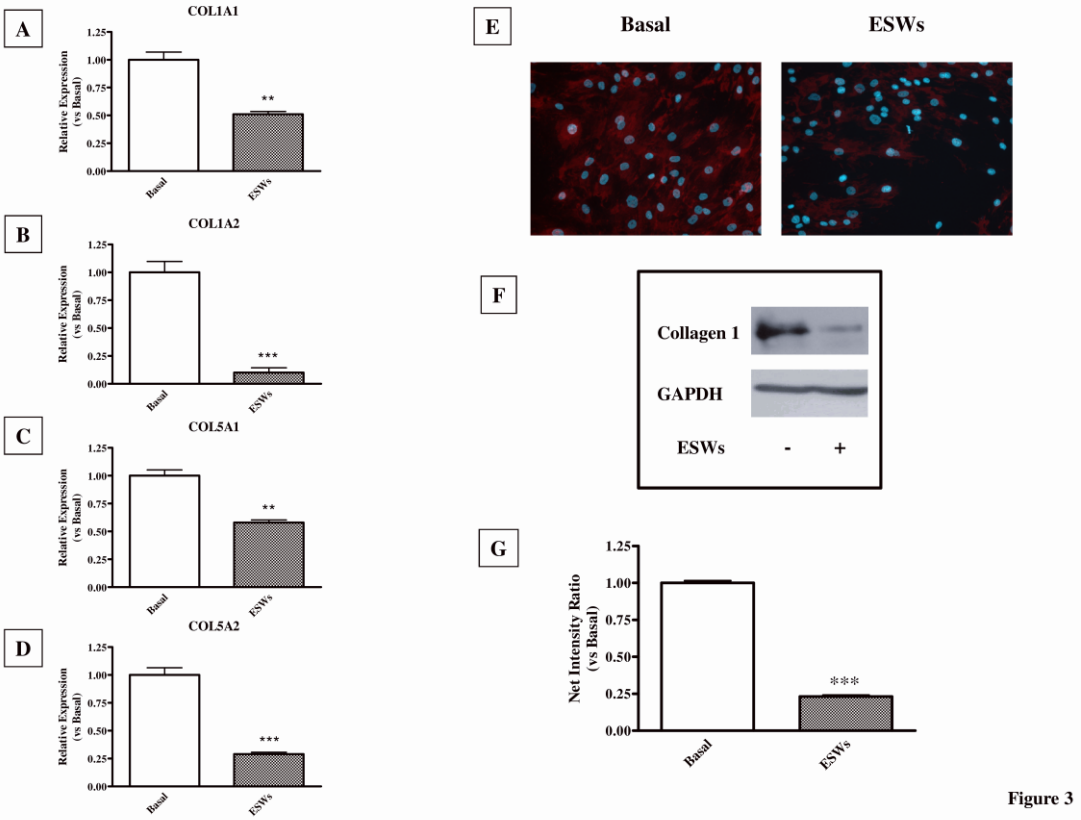
A
COL1A1
Relative Expression (vs Basal)
1.25
1.00
0.75
0.50
0.25
0.00
**
Basal
ESWs
B
COL1A2
Relative Expression (vs Basal)
***
C
COL5A1
**
D
COL5A2
***
E
Basal
ESWs
F
Collagen 1
GAPDH
ESWs - +
G
Net Intensity Ratio (vs Basal)
***

Figure 3

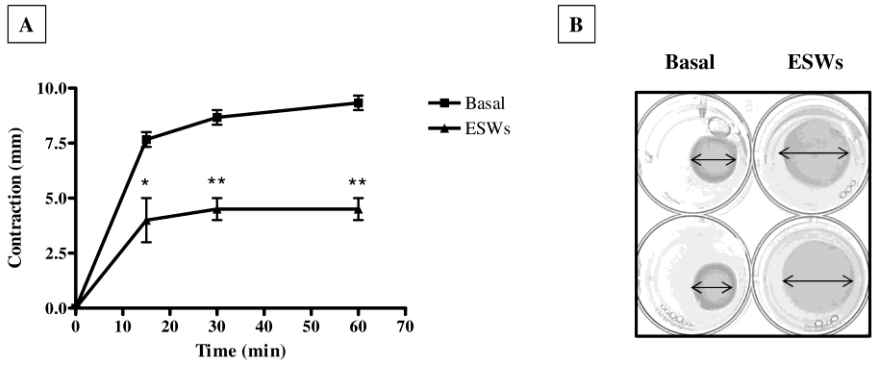
A
B
Basal
ESWs
10.0
7.5
5.0
2.5
0.0
Contraction (mm)
0
10
20
30
40
50
60
70
Time (min)
Basal
ESWs
*
**
**

Figure 4

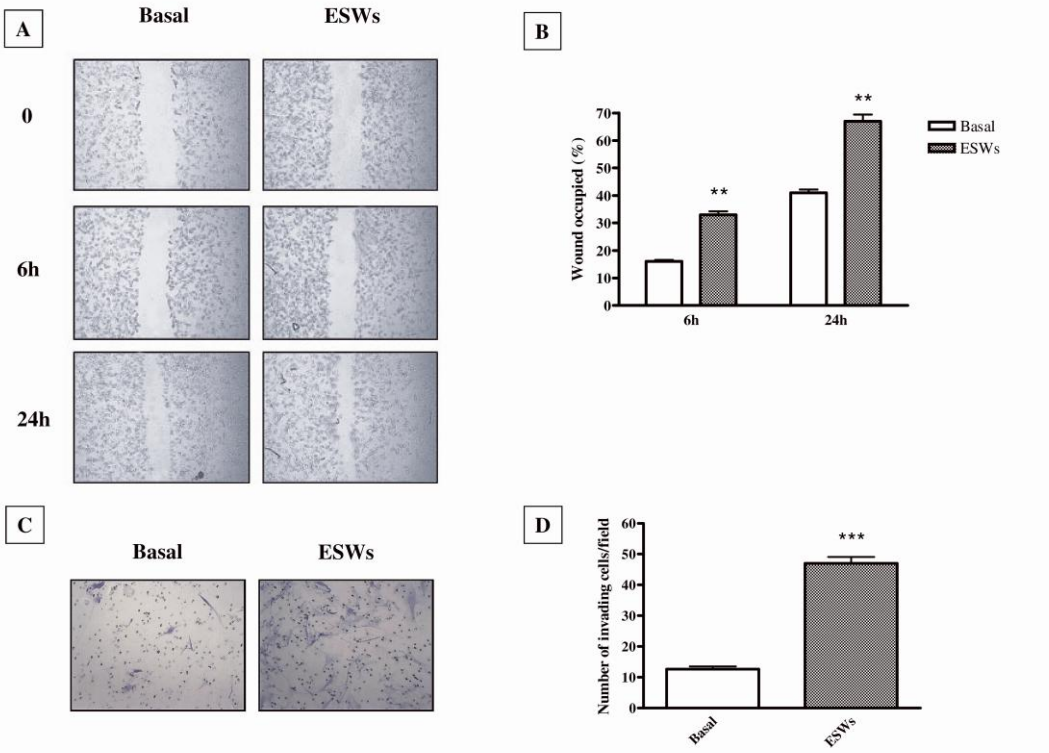
A
Basal
ESWs
0
6h
24h
B
Wound occupied (%)
70
60
50
40
30
20
10
0
**
**
6h
24h
Basal
ESWs
C
Basal
ESWs
D
Number of invading cells/field
60
50
40
30
20
10
0
***
Basal
ESWs

Figure 5

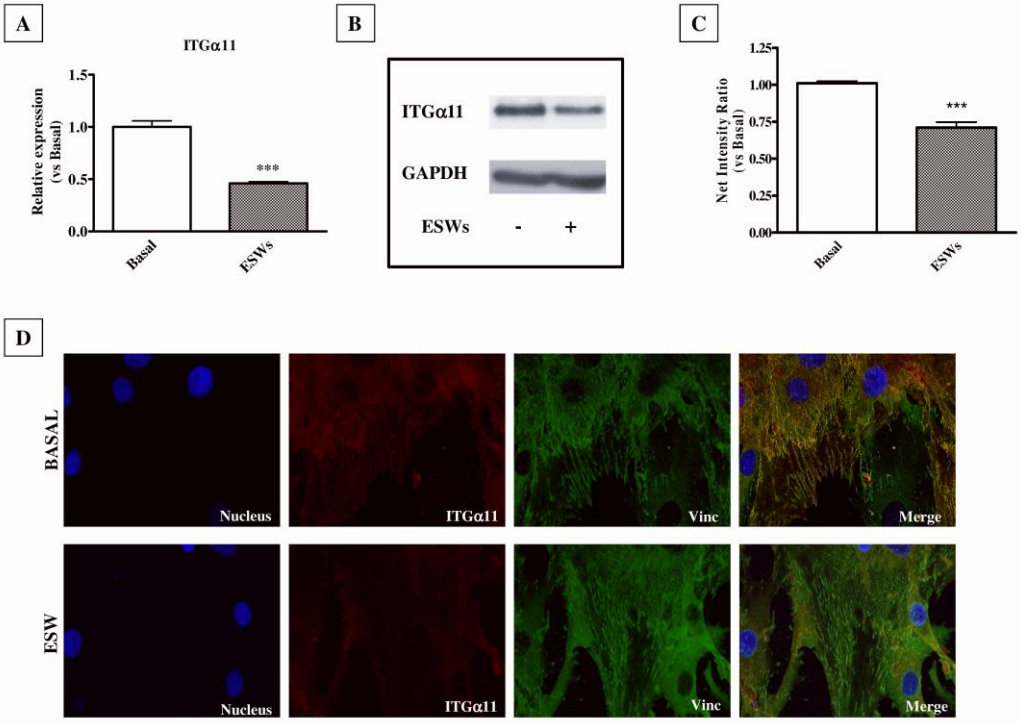
A
ITGα11
Relative expression (vs Basal)
1.5
1.0
0.5
0.0
***
Basal
ESWs
B
ITGα11
GAPDH
ESWs - +
C
Net Intensity Ratio (vs Basal)
1.25
1.00
0.75
0.50
0.25
0.00
***
Basal
ESWs
D
BASAL
ESW
Nucleus
ITGα11
Vinc
Merge
Nucleus
ITGα11
Vinc
Merge

Figure 6

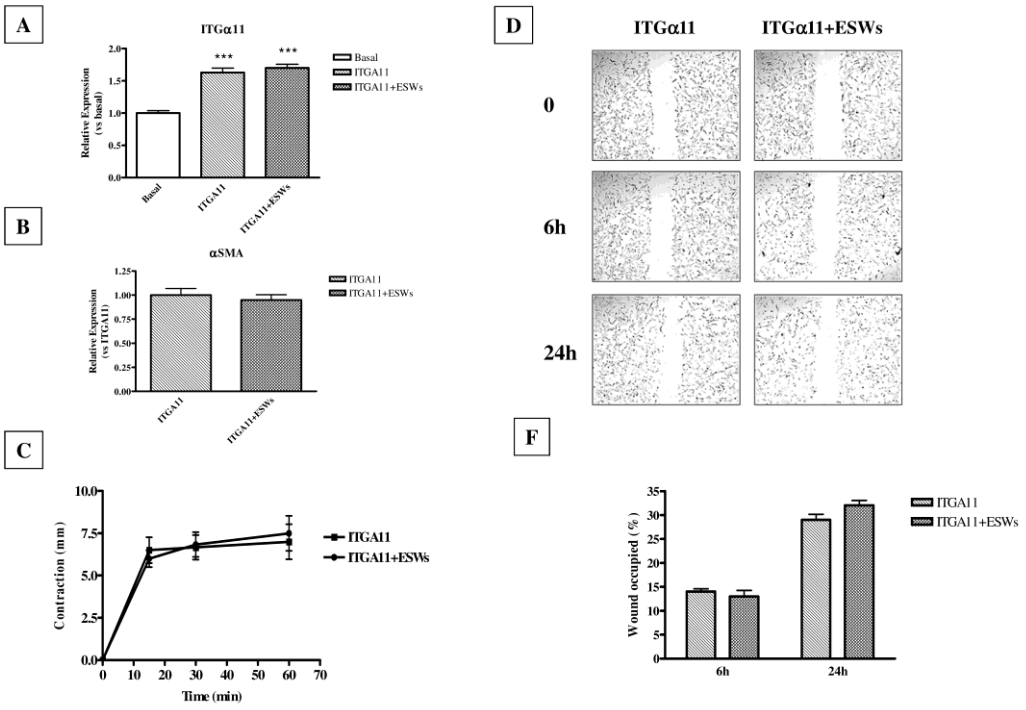
A
ITGα11
Relative Expression (vs basal)
2.0
1.5
1.0
0.5
0.0
***
***
Basal
ITGA11
ITGA11+ESWs
B
αSMA
Relative Expression (vs ITGA11)
1.25
1.00
0.75
0.50
0.25
0.00
ITGA11
ITGA11+ESWs
C
Contraction (mm)
10.0
7.5
5.0
2.5
0.0
0
10
20
30
40
50
60
70
Time (min)
ITGA11
ITGA11+ESWs
D
ITGα11
ITGα11+ESWs
0
6h
24h
F
Wound occupied (%)
35
30
25
20
15
10
5
0
6h
24h
ITGA11
ITGA11+ESWs

Figure 7

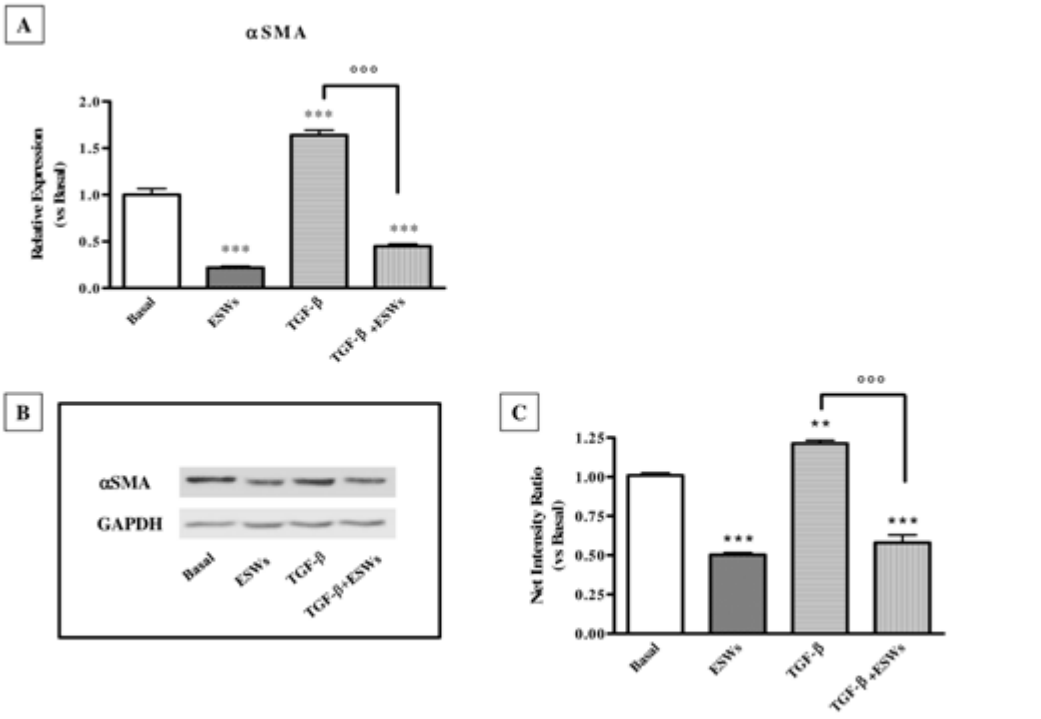
A
αSMA
Relative Expression (vs Basal)
2.0
1.5
1.0
0.5
0.0
***
***
***
°°°
Basal
ESWs
TGF-β
TGF-β +ESWs
B
αSMA
GAPDH
Basal
ESWs
TGF-β
TGF-β+ESWs
C
Net Intensity Ratio (vs Basal)
1.25
1.00
0.75
0.50
0.25
0.00
**
***
***
°°°
Basal
ESWs
TGF-β
TGF-β +ESWs

Figure 8

Table 1. Mesenchymal stem cell marker expression after ESW treatment. The percentage of CD antigen-positive cells in a population of 10000 cells is reported as mean of three different experiments.

	Basal	Days after ESW treatment			
		3	7	14	21
CD 13	97.2 ± 3.5	95.0 ± 5.0	97.0 ± 2.2	97.0 ± 0.6	99.5 ± 0.6
CD 44	98.8 ± 1.1	99.5 ± 0.5	96.3 ± 1.6	97.0 ± 2.2	96.5 ± 3.7
CD 90	92.6 ± 2.8	88.6 ± 2.1	94.6 ± 2.8	95.0 ± 1.9	96.1 ± 1.6
CD 105	96.5 ± 3.7	99.5 ± 4.9	96.8 ± 4.2	94.7 ± 6.3	93.8 ± 2.2

Table S1 Primers for real-time PCR

Runx2	Sense: 5’- CGG AGT GGA CGA GGC AAG AG -3’ Antisense: 5’- AGG CGG TCA GAG AAC AAA CTA GG -3’
PPARγ	Sense: 5’- TGT CGG TTT CAG AAA TGC CTT GC -3’ Antisense: 5’- GAG GTC AGC GGA CTC TGG ATT C -3’
SOX2	Sense: 5’- ATG GGT TCG GTG GTC AAG TCC -3’ Antisense: 5’- CTG GAG TGG GAG GAA GAG GTA AC -3’
OCT4	Sense: 5’- AGC AGG AGT CGG GGT GG -3’ Antisense: 5’- CTG GGA CTC CTC CGG GTT -3’
KLF4	Sense: 5’- CCA TTACCA AGA GCT CAT GCC -3’ Antisense: 5’- GGG CCA CGA TCG TCT TCC -3’
NANOG	Sense: 5’- GAG ATG CCT CAC ACG GAG ACT G -3’ Antisense: 5’- GGT TGT TTG CCT TTG GGA CTG G -3’
αSMA	Sense: 5’- GGA GCA GCC CAG CCA AGC -3’ Antisense: 5’- AGA GCC CAG AGC CAT TGT CAC -3’
COL1A1	Sense: 5’- CAA GAC GAA GAC ATC CCA CCA ATC -3’ Antisense: 5’- GGC AGG GCT CGG GTT TCC -3’
COL1A2	Sense: 5’- ATG GAT GAG GAG ACT GGC AAC C -3’ Antisense: 5’- GGA AGG GCA GGC GTG ATG G -3’
COL5A1	Sense: 5’- CAG CAC CGC CGA CAC CTC -3’ Antisense: 5’- CTC CAA GTC ATC CGC ACC TTC C -3’
COL5A2	Sense: 5’- CCA GGA AGA AGA CGA GGA TGA AGG -3’ Antisense: 5’- GGT CGG CAC AGT CCA GCA C -3’

bFGF	Sense: 5’- AGA AGA GCG ACC CTC ACA TCA AG -3’ Antisense: 5’- TAG CCA GGT AAC GGT TAG CAC AC -3’
ITGα3	Sense: 5’- CCT ATT CCT CCG AAC CAG CAT CC -3’ Antisense: 5’- CCA CCA GCA CCA GCC ACA G -3’
ITGα5	Sense: 5’- CGG GCT CCT TCT TCG GAT TCT C -3’ Antisense: 5’- CAC TCC TGG CTG GCT GGT ATT AG -3’
ITGαV	Sense: 5’- TAG CGT ATC TGC GGG ATG AAT CTG -3’ Antisense: 5’- GGC GTG AAC TGG TTA AGA ATG GG -3’
ITGα11	Sense: 5’- GCA GGC AGT GAC AGT AAT GA GC -3’ Antisense: 5’- CGT ATT TGA GGT GGA AGC GTA AGG -3’
β-ACT	Sense: 5’-GCG AGA AGA TGA CCC AGA TC- 3’ Antisense: 5’- GGA TAG CAC AGC CTG GAT AG-3’
L13A	Sense: 5’-GCA AGC GGA TGA ACA CCA ACC-3’ Antisense: 5’-TTG AGG GCA GCA GGA ACC AC-3’
RPLPO	Sense: 5’-CGA CAA TGG CAG CAT CTA CAA CC-3’ Antisense: 5’-CAC CCT CCA GGA AGC GAG AAT G-3’